JOURNAL OF MATERIALS SCIENCE 21 (1986) 3810–3816

Microstructure of porous anodic oxide films on aluminium

K. WADA, T. SHIMOHIRA
National Institute for Research in Inorganic Materials, Namiki, Sakura-mura, Niihari-gun, Ibaraki 305, Japan

M. YAMADA
College of Science and Technology, Nihon University, Kanda-Surugadai, Chiyoda-ku, Tokyo 101, Japan

N. BABA
Tokyo Metropolitan University, Fukasawa, Setagaya-ku, Tokyo 158, Japan

Microstructure of porous anodized films of aluminium prepared in sulphuric acid solution are different from those prepared in an oxalic or phosphoric acid solution. Transmission electron microscopy reveals a multilayer or higher order structure in the former films. Infrared spectra and specific surface area were also studied for these films and new functional properties of the films suitable for new materials were found. In contrast to the fibrous colloidal structure in the cells and barrier layer in the conventional films anodized in a sulphuric acid solution at d.c. 15 V, a network structure is formed in the cells and barrier layer in the hard films prepared at higher voltage of d.c. 25 V. The microstructure changes according to the anodizing conditions. A new model for these sulphuric acid films is presented, i.e. the cell walls are constructed from five layers and the fracture of the films occurs at the centre of the cell walls. Centre barrier layer (4 to 6 nm in thickness) composed of aluminium oxide of high crystallinity was found in a barrier layer at the bottom of the pore, and the thickness is independent on the applied voltage of the anodizing. Increase in thickness of the barrier layer due to applied voltage is governed by that of the outer barrier layer.

1. Introduction

It is well known that a porous anodized film is formed on the surface of aluminium by anodization in acid or alkaline solutions [1–5]. By using these porous structures and hardness, these films have been applied to many industrial purposes. Recently, many investigations have been made on new application of these films by studying the porous microstructures of the films [6, 7].

Among many models proposed so far for the porous structure of the films, Keller *et al.* [3] and Akahori [5] presented typical models. Thompson *et al.* [8, 9], Takahashi *et al.* [10] and Fukuda [11] showed new models constructed from cells and barrier layers, having inhomogeneous chemical composition. Their models were for oxalic and phosphoric acid films (hereafter the films are specified by the name of the electrolyte used). Recently, Thompson *et al.* [12] irradiated the cross-section of the phosphoric acid film with an electron beam and observed the irradiation time dependence of the microstructure of the section with a transmission electron microscope (TEM) and concluded the formation of special microstructures in the cells and barrier layer. Murphy and Michelson [13] studied sulphuric acid films chemically and reported that the cells and barrier layer are composed of hydrous and hydrated oxide particles. No report supporting this model has been found so far.

Considering the effect of electron beam and heat damages reported recently, the present authors have found the change of ordered microstructure (hereafter this is called as higher order structure [14]) in the cross-section of the sulphuric acid film containing a larger amount ($\sim 15\%$) [15] of adsorbed water compared with the phosphoric or oxalic acid film, and reported that this structure change is a typical characteristic of the sulphuric acid film. From the finding of the fibrous colloid structure in the sulphuric acid film prepared by conventional methods, we concluded that the microstructure of this film does not agree with that of the phosphoric acid film model [12].

The purpose of the present study is (a) further confirmation of the existence of the higher order structure in the sulphuric acid film prepared by the conventional method; and (b) elucidation of the effect of electrolytic condition on the microstructure of the hard type sulphuric acid film (hereafter called the hard film) prepared by applying a high voltage by the observation of new microstructure in this film. To this end, we immersed and dissolved these films in a warm sulphuric acid solution and measured the change in chemical compositions and specific surface area during the dissolutions and also the change in the microstructure of the cells and barrier layer and finally discussed the model of the cross-section structure of the sulphuric acid film.

0022–2461/86 $03.00 + .12

2. Experimental details

2.1. Anodic oxidation (anodization)

The sample used was aluminium foil of 100 μm in thickness and 99.3% in purity. Pretreatment was made by wiping the surface of the foil with cotton containing trichloroethylene.

Anodization was carried out in an aqueous solution of sulphuric acid (1 mol dm^{-3}) at d.c. 15 V for 5 min (20° C) for conventional films, and at 25 V for 15 min or 60 min (2 to 5° C) for hard films, both at constant voltage. For the purpose of comparison, anodizations in phosphoric acid and oxalic acid were also carried out at a constant voltage, i.e. 15 V for 9 min (20° C) for the former solution of 0.2 mol dm^{-3} and 15 V for 50 min (21° C) for the latter solution of 0.3 mol dm^{-3}.

2.2. Chemical dissolution

The films were dissolved in aqueous solution of sulphuric acid (1 mol dm^{-3}) at 40° C [16] for 10 and 20 min in the ordinary case and for 18, 30, 32 and 40 min in the case of the hard films.

2.3. Specific surface area

To know the change in surface area of the sulphuric acid films, which were prepared by the ordinary method (d.c. 15 V), by chemical dissolution, the specific surface area was measured in a vacuum (ca. 1×10^{-5} torr) at 200° C by BET (Brunauer-Emmett-Teller) method using the apparatus made by Makuhari Kaguku garasu Seisakusyo Co.

2.4. Observations with TEM

The films were embedded in epoxy resin and cured at 60° C for 24 h. Then the specimens (30 to 40 nm in thickness) which were prepared by cutting the film with an ultramicrotome made by LKB Co. were scooped with a copper net for the electron microscope (H-500, 100 kV made by Hitachi Seisakusyo). Some of the specimens were prepared by the replica method.

2.5. Infrared spectra

Changes in i.r. spectra of the hard film by the chemical dissolution was measured by the three times reflection method using EP1-G3 (Hitachi Seisakusyo). The anodized specimens were kept in a desiccator after natural drying for 20 min.

3. Results and discussion

3.1. Changes in the specific surface area and microstructure of the sulphuric acid film

In general, the transmission electron micrographs of the fracture surface perpendicular to the film surface show many cylindrical structures having pores (diameter 10 to 30 nm) in each cylinder. From these micrograhs of the fracture surface of the phosphoric and oxalic acid films Booker *et al.* [4] inferred three ways (A–A, B–B, C–C in Fig. 1) for fracture of the film. Their consideration may be valid if there is aluminium oxide of high crystallinity in the centre of the cells as shown by a model of Thompson *et al.* [6, 7]. We confirmed the three kinds of fracture surfaces shown in Fig. 1 for the sulphuric acid films (Fig. 2) prepared by conventional conditions. In the case of the hard film

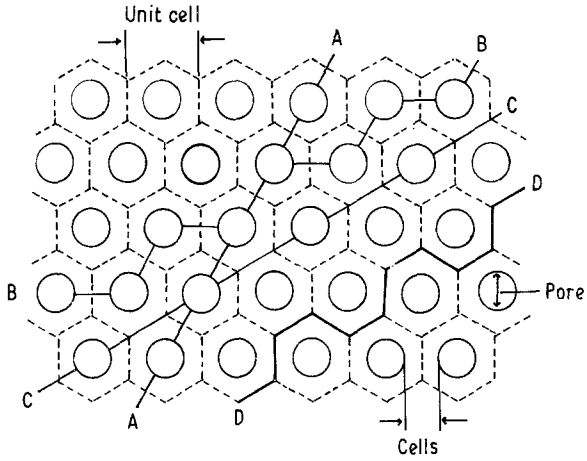

Figure 1 Fracture models of porous anodic oxide films. A–A, B–B and C–C: Booker *et al.* [4]. D–D: present authors.

(25 V) the fracture was found to occur along the D–D line in Fig. 1, i.e. along the centre of the cells (Fig. 3). These results suggest that the microstructure of the sulphuric acid film differs from that of the oxalic and phosphoric acid films, i.e. the former films may have a new microstructure, the higher order structure, which is not in the latter films.

TEM revealed the following: by 15 min chemical dissolution of outer cell layer (OC in Fig. 4 which shows a new model proposed here by us) in the cells of the conventional sulphuric acid film (Fig. 2), there appear multilayers constructed by regular colloidal fibre structure (hereafter this is also called a higher order structure) in Fig. 5 growing from the bottom of the pores. By further dissolution, the outer cell layer

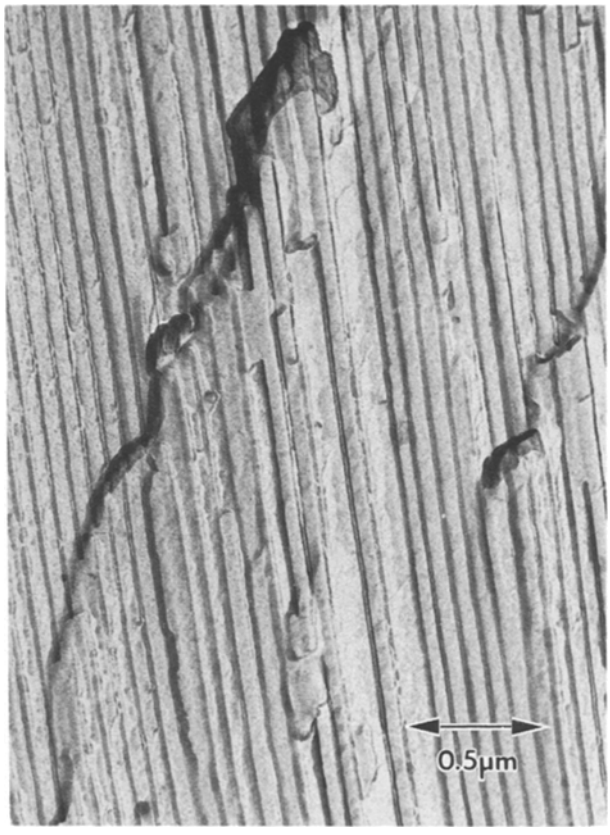

Figure 2 Side view of the fracture surface of sulphuric acid film prepared with the conventional condition (15 V), (replica method).

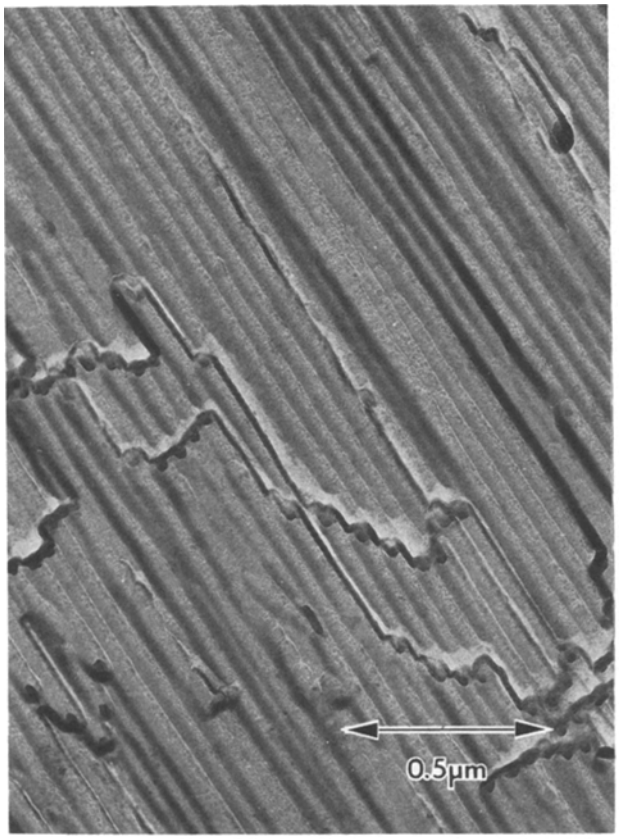

Figure 3 Side view of the fracture surface of hard film prepared with high voltage (25 V), (replica method).

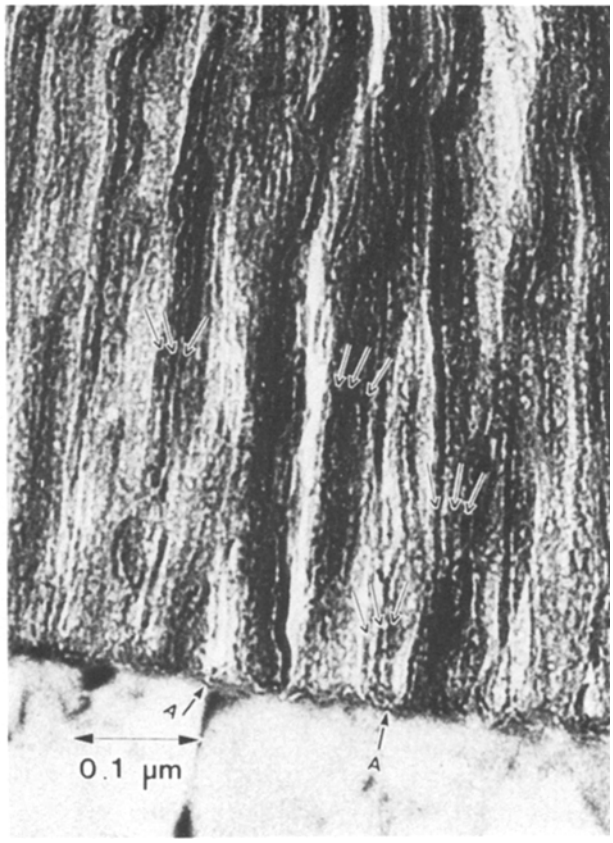

Figure 5 TEM image of the cross-section of the conventional sulphuric acid film (15 V) showing the colloidal fibre structures.

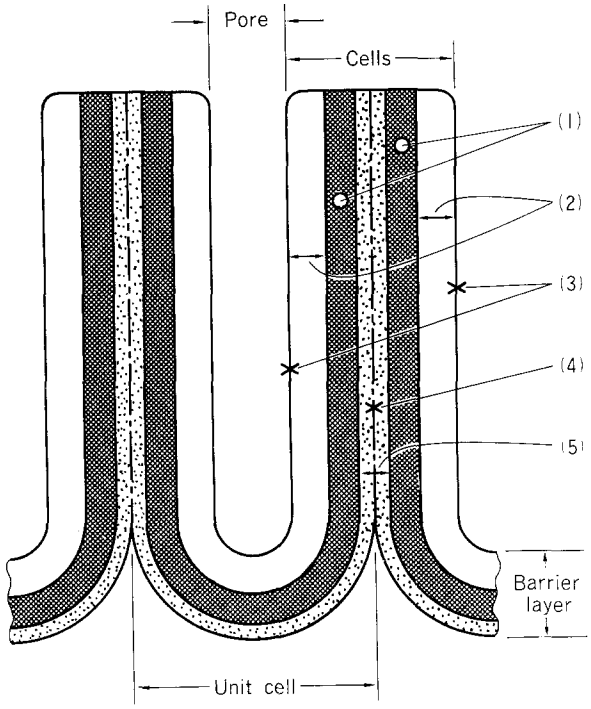

(1) Centre barrier layer(CB)
(2) Outer cell layer(OC)
(3) Outer cell wall(OCW)
(4) Centre of inner cell layer(CIC)
(Inner cell wall:ICW)
(5) Inner cell layer(IC)
(Boundary layer)

Figure 4 Multilayer model of cross-section of sulphuric acid film.

(OC in Fig. 4) and the inner cell layer (IC in Fig. 4) disappear and centre barrier layers (CB in Fig. 4) of 4 to 6 nm in thickness remain in the cells.

To confirm the higher order structure in the conventional film with another method, the effect of progress of the chemical dissolution on the specific surface area of the film prepared by anodization for 80 min was

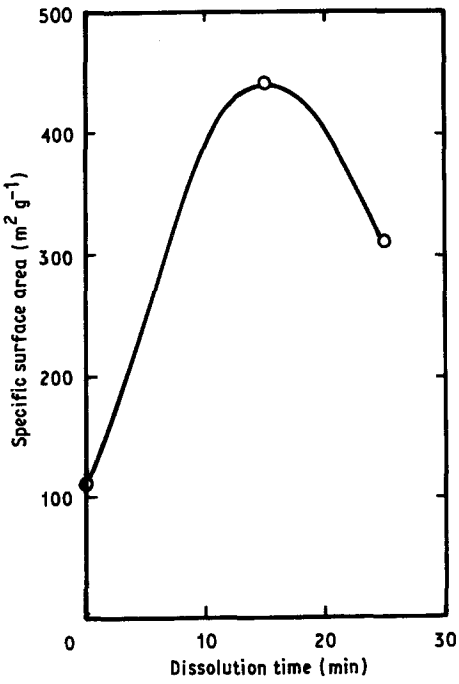

Figure 6 Effect of dissolution time on specific surface area of the conventional sulphuric acid film (15 V).

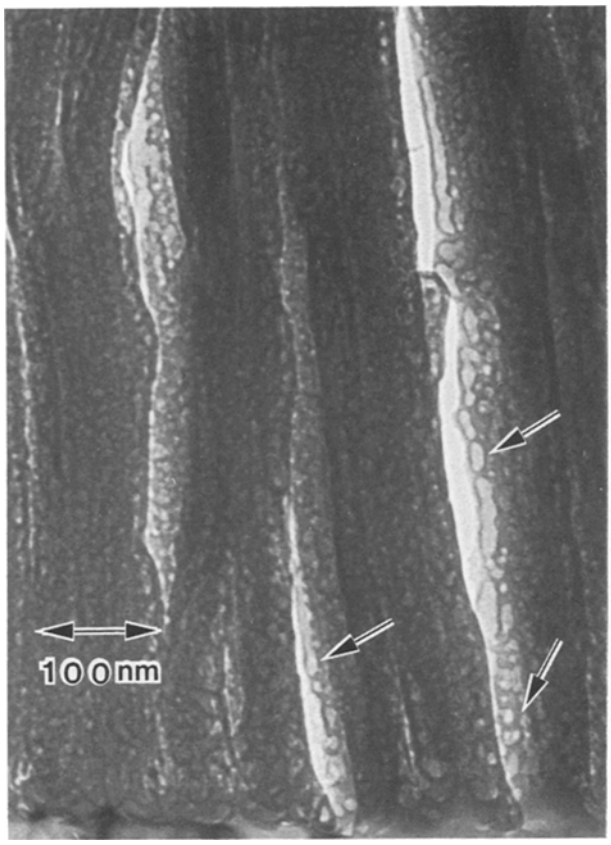

Figure 7 TEM image of the cross-section of the hard film (25 V) showing the network structure.

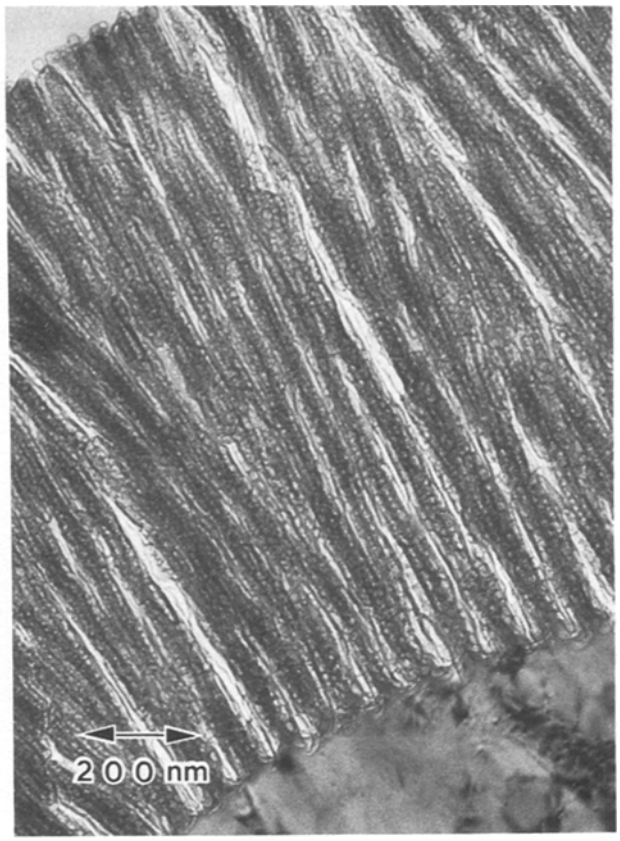

Figure 8 TEM image of the cross-section of the hard film showing the fibre structure after chemical dissolution (18 min).

measured by the BET method (Fig. 6). The figure shows that the original area ($112\,m^2\,g^{-1}$) increases to a maximum value of $442\,m^2\,g^{-1}$ after the chemical dissolution for 15 min, which coincides with the time of maximum appearance of the higher order structure shown in Fig. 5. After this time, with increasing dissolution the area decreases to $\sim 300\,m^2\,g^{-1}$ (after 24 min).

These results of the specific surface area imply that the specific surface area of the sulphuric acid film depends not only on the increase of the pore diameter but also on the higher order structure in the cells.

3.2. Change in higher order structure of the hard film

Fig. 7 shows transmission electron micrograph of the film section perpendicular to the surface of the hard film before the chemical dissolution. The film was prepared by anodization at d.c. 25 V for 15 min. It is worth mentioning that contrary to the conventional film, the above film without chemical dissolution shows a typical network structure (hereafter this is also called a higher order structure). Sizes of the network seen with bright contrast and shown by arrows are 4 to 13 nm and those with dark contrast are 4 to 8 nm which are close to the size of the centre barrier layer (CB in Fig. 4) of the conventional films. Thickness of the barrier layer formed at 25 V may be expected as 25 to 35 nm from the conventional theory, but the figure does not show the layer having such a uniform thickness. The higher order structure of the hard film is easily formed in the cells at the initial stage of the chemical dissolution.

Fig. 8 shows the film section parallel to the surface of the film obtained by the chemical dissolution (18 min) of the film shown in Fig. 7. Number of the network structure in Fig. 8 is larger than that in Fig. 7 and the fibre structures are seen more clearly in Fig. 8. Sizes of these fibre structures are 4 to 8 nm which are

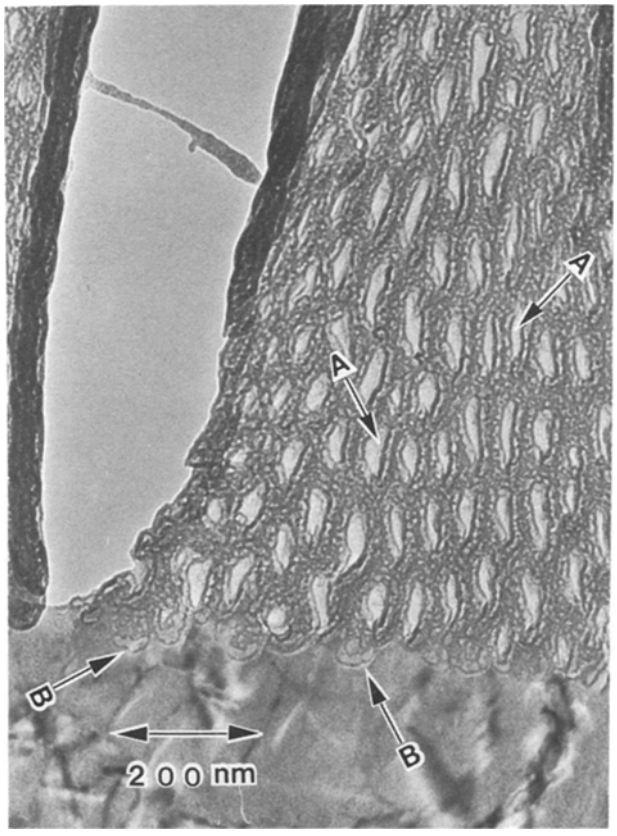

Figure 9 TEM image of the hard film of an ultramicrotomed film section parallel to the film surface after 18 min chemical dissolution.

almost independent of the chemical dissolution. Fig. 9 shows an ultramicrotomed film section parallel to the surface of the film shown in Fig. 8. The tilted section of the aluminium substrate seen at the bottom of the pore in Fig. 9 indicates imperfect parallelism of the cutting direction. Diameters of the pores are enlarged by the dissolution and the pores are deformed in a spindle shape by the stress of the cutting. Thicknesses of the cells are distributed within ~26 to 40 nm. Three layer structures (6 to 8 nm in thickness) are seen by dark lines (arrows A) in the thin portions of the cells. These multilayers (five layers) constructed from three black layers and two inter layers are similar to that in the conventional films [14]. In the thick portion of the cells, however, due to incomplete dissolution, the network structure remains to form more complicated multilayers. In the boundary between the film and aluminium substrate, there are many network structures (size 4 to 6 nm) shown by dark lines (arrows B). The thickness of this structure is a little thinner than the centre barrier layer (CB in Fig. 4) of 6 to 8 nm thickness in the cells.

Fig. 10 shows a film section parallel to the surface of the hard film after 30 min chemical dissolution. Though the figures of the pores are a little deformed by the stress of cutting, there are typical multilayers (five layers as shown by the arrows) showing the progress of the chemical dissolutions, i.e., the enlargement of the pore diameters up to 22 to 35 nm and decrease of thickness of the outer cell layer (OC in Fig. 4) to 26 to 29 nm.

To construct the final models for the cells and barrier layers of the sulphuric acid film, a micrograph of the hard film section perpendicular to the film surface was taken after the chemical dissolution for 32 min (Fig. 11). The figure shows the enlargement of the pore diameters up to 23 to 42 nm, i.e. the widening of the distribution of the pore diameters by chemical dissolutions. The figure also shows the centre barrier layers (CB in Fig. 4) of 4 to 8 nm in thickness (arrows A), i.e. the widening of the distribution of the thickness.

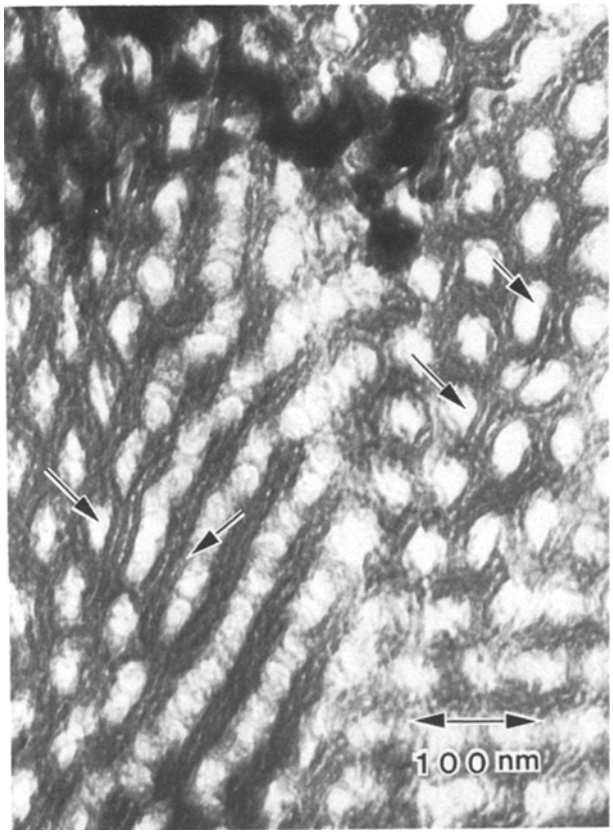

Figure 10 TEM image of the hard film of an ultramicrotomed film section parallel to the film surface after 30 min chemical dissolution.

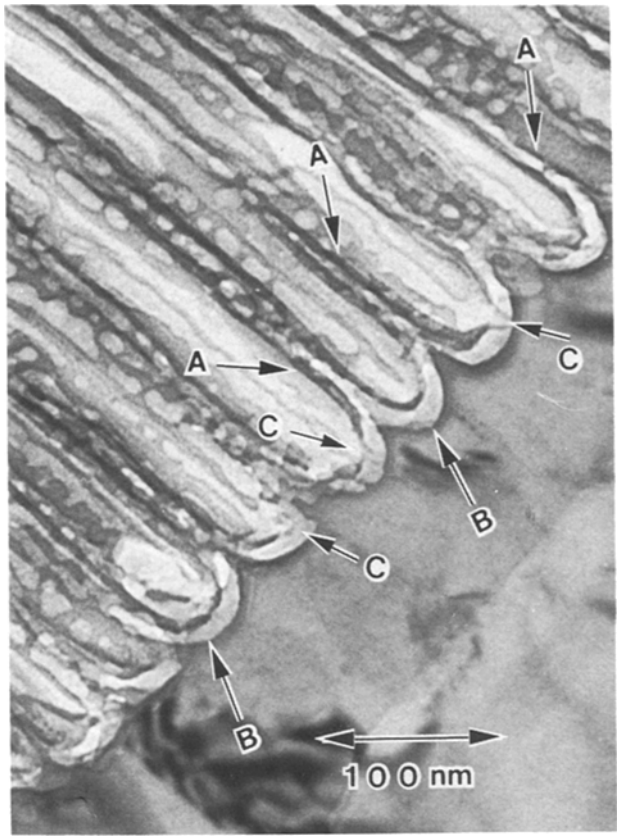

Figure 11 TEM image of the cross-section of the hard film showing the centre barrier layer after 32 min chemical dissolution.

At this stage of the chemical dissolution, all of the outer cell layers (OC in Fig. 4) are dissolved away and the cells are constructed by the remaining two centre barrier layers (CB in Fig. 4) and one inner cell layer (IC in Fig. 4). The cells show a higher order structure composed of these three layers. Since the outer cell layer (OC in Fig. 4) is easily damaged by chemical agents the film, immediately after the anodization, might show almost seven layers. Besides this multilayer, due to adsorbed water and anions, the film takes a chemically inhomogenized structure.

These results clearly show that the fracture of the film, which was prepared at high voltage and high current density, occurs at the layer between the two centre barrier layers (CB in Fig. 4). Therefore, the sulphuric acid film is constructed not only from a structure containing an aluminium oxide layer of high crystallinity in the centre of the cells, i.e. the conventional model, but also from the above mentioned two layers of high crystallinity and an inner cell layer (IC in Fig. 4) between these two oxide layers. The new model presented in Fig. 4 can well explain the observation of the fracture surface which does not show the pores mentioned before.

Fig. 11 shows three defects (arrow C), which reach

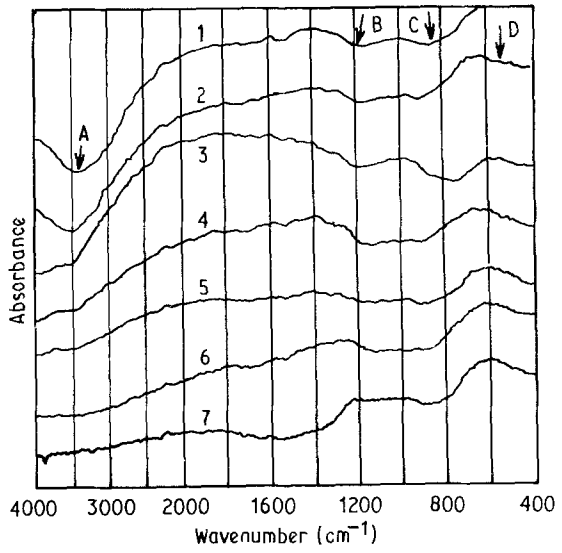

Figure 12 Variation of i.r. spectra with the duration of chemical dissolution of the hard film. Time (min): 1, 0; 2, 10; 3, 20; 4, 30; 5, 40; 6, 50; 7, aluminium foil.

the aluminium substrate. This finding supports the consideration of Fukuda *et al.* [17] who suggested these gaps, which reach the aluminium substrate, in the barrier layer of the film prepared in 13 M sulphuric acid solution.

3.3. Dependence of the chemical dissolution on i.r. spectra of the hard film

Curves 1 to 6 in Fig. 12 show the i.r. spectra of the hard film chemically dissolved for 0, 10, 20, 30, 40 and 50 min, respectively. Curve 7 is the spectrum for the surface of aluminium foil before anodization. The i.r. adsorption band 3660 to 2940 cm^{-1} (arrow A) is assigned to the AlO↔H stretching vibration and shows the existence of adsorbed water [18]. This absorption decreases with the progress of the chemical dissolution. These results suggest that the chemical dissolutions of the hard film proceed slowly because the amount of the adsorbed water is smaller and the crystallinity of the film is higher in the hard film than in the conventional film. The tendency of decrease of the adsorbed water due to the outer cell wall (OCW in Fig. 4) dissolutions shows an intrinsic change of the chemically adsorbed water in the film. Contrary to this tendency, i.r. absorption for adsorbed water in the conventional film increases with the progress of the chemical dissolution [14]. This trend, however, can not be considered to be an intrinsic behaviour of the adsorbed water in the conventional film but is considered to be a temporary behaviour of the physically adsorbed water on the outer cell wall (OCW in Fig. 4).

i.r. absorption in the vicinity of 1150 cm^{-1} (arrow B) is assigned to SO_4^{2-} ions and implies the existence of anions from the electrolyte in the film. This absorption does not show remarkable decreases with the progress of the chemical dissolution.

The absorption near 900 to 825 cm^{-1} (arrow C) corresponds to the stretching vibration of Al↔OH and shows the existence of a hydrate of aluminium in the film [18]. Intensity of these absorptions are almost independent of the chemical dissolution in the case of the hard film. The absorptions (arrow D) below ~800 cm^{-1} corresponding to the stretching vibration of Al↔OAl show the existence of a polymeric substance having a network structure [18]. For the hard film, the change in this absorption due to the chemical dissolution is very little and is hardly observable.

As mentioned above, the change in i.r. absorption due to the chemical dissolution of the hard film is different from that of the conventional film. This result shows the difference of the chemical composition and higher order structure between these two films.

3.4. Model of the sulphuric acid film

From Figs 3 and 11, it is clear that the fracture of the sulphuric acid film occurs at the centre of the cells. This mechanism is not included in the three ways of the fracture proposed by Booker *et al.* [4]. The models for these fracture lines are shown in Fig. 1, in which A–A, B–B and C–C are the lines reported by Booker *et al.* and D–D is that proposed by us. This D–D fracture line was already inferred by Baily and Wood [19] for oxalic acid films without experimental confirmation. According to our investigation, this line is specific for sulphuric acid films and was not found for oxalic acid films. Usually, it is shown that the porous structure containing the cells and barrier layers depends on the kind of electrolyte used. To check this estimation we observed the ultramicrotomed specimens of the phosphoric and oxalic acid films in the same conditions as in the case of the sulphuric acid film. Since these two sections did not show any special microstructures, the higher order structure is considered to be grown only in the sulphuric acid film.

In the case of the sulphuric acid film, though the films are prepared in the same electrolyte the higher order structure in the film depends on the conditions of electrolysis. Thus, the model of the film should be discussed case by case based on the correct information on the conditions of electrolysis, rather than proposing a unified model for various cases, i.e. one must consider different models for different films. The new model shown in Fig. 4, is presented here to explain the properties of the hard and conventional films observed in common.

The thickness of the actual centre barrier layer (CB shown in Fig. 4) is of course not uniform. In general, the thickness of the bottom barrier layer might increase with the rate of 1 to 1.4 nm V^{-1} as already reported [20, 21], but there remains a question whether this consideration holds in the case when a higher voltage (Fig. 7) is applied. This increase in thickness of the barrier layer occurs only for the outer cell layer (OC in Fig. 4), i.e. the thickness of the centre barrier layer (CB in Fig. 4) is almost constant (4 to 6 nm) independent of the applied voltage.

4. Conclusions

Formation of a special regular higher order structure was found in the cells and barrier layer of the sulphuric acid film. This structure is formed only in the sulphuric acid film and not in the phosphoric and oxalic acid films. On the observation of the formation of this structure, the effects of the adsorbed water and

the damage of electron beam bombardment including heating effects are also taken into consideration. The microstructure and the new higher order structure appeared before and/or after the chemical dissolutions of the film were examined by TEM, i.r. spectra, and the measurements of specific surface area and the following conclusions were obtained.

1. From the findings that the specific surface area of the film prepared by the ordinary method shows a maximum value after the chemical dissolution of the cells, it is considered that the specific surface area depends not only on enlargement of the pores in the porous layer, but also on the existence of the higher order structure in the cells.

2. When a higher voltage of electrolysis is applied, the fracture occurs at the centre of the cells, i.e. at the boundary layer (IC in Fig. 4) between the two centre barrier layers (CB in Fig. 4).

3. It is worth mentioning that clear network structure is usually found in the hard film.

4. In the barrier layer there is a centre barrier layer (CB in Fig. 4) of thickness 4 to 6 nm which is constant independent of the applied voltage.

5. Increase of the thickness of the barrier layer by the applications of voltage is due to the increase of the thickness of the surface layer (OC in Fig. 4) of the barrier layer.

6. The thickness of the barrier layer of the sulphuric acid film prepared by applying high voltage can not be explained by the usual rate (1 to 1.4 nm V^{-1}) of the increase of thickness as already reported.

References

1. T. RUMMEL, *Z. Physik.* **99** (1936) 518.
2. W. BAUMANN, *ibid.* **102** (1936) 59.
3. F. KELLER, M. S. HUNTER and D. L. ROBINSON, *J. Electrochem. Soc.* **100** (1953) 411.
4. C. J. L. BOOKER, J. L. WOOD and A. WALSH, *Brit. J. Appl. Phys.* **8** (1957) 347.
5. H. AKAHORI, *J. Electronmicroscopy* **10** (1961) 175.
6. M. YAMADA and K. ITABASHI, in Proceedings of the 8th International Congress on Catalysis, West Berlin, West Germany (1984) IV, 835-846.
7. K. ITAYA, S. SUGAWARA, K. ARAI and S. SAITO, *J. Chem. Eng. Jpn.* **17** (1984) 514.
8. G. E. THOMPSON, R. C. FURNEAUX, J. S. GOODE and G. C. WOOD, *Trans. Inst. Met. Finish.* **56** (1978) 159.
9. G. E. THOMPSON, R. C. FURNEAUX, G. C. WOOD, J. A. RICHARDSON and J. S. GOODE, *Nature* **272** (1978) 433.
10. H. TAKAHASHI and M. NAGAYAMA, *Nippon Kagaku Kaishi* (1974) 453.
11. Y. FUKUDA, *ibid.* (1974) 1868.
12. G. E. THOMPSON and G. C. WOOD, *Electrochim. Acta* **27** (1982) 1623.
13. J. F. MURPHY and C. E. MICHELSON, in Proceedings of the Conference on Anodizing Aluminium, Nottingham, England (1961) 83.
14. K. WADA, Y. MATSUI, Y. SEKIKAWA and T. SHIMOHIRA, *Nippon Kagaku Kaishi* (1984) 893.
15. N. D. PULLEN, *Electrodeposit Technol. Soc.* **15** (1939) 68.
16. M. NAGAYAMA and K. TAMURA, *Denkikagaku* **36** (1968) 34.
17. Y. FUKUDA, T. FUKUSHIMA and M. NAGAYAMA, *Kinzoku Hyoumen Gigyutsu* **35** (1984) 513.
18. G. A. DORSEY, *J. Electrochem. Soc.* **113** (1966) 169.
19. G. BAILY and G. C. WOOD, *Trans. Inst. Met. Finish.* **52** (1974) 187.
20. G. C. WOOD, J. P. O'SULLIVAN and B. VASZKO, *J. Electrochem. Soc.* **115** (1968) 618.
21. M. NAGAYAMA, H. TAKAHASHI and M. KOUDA, *Kinzoku Hyoumen Gigyutsu* **30** (1979) 438.

Received 22 October
and accepted 20 December 1985